

# Theory of non-Gaussianity in warm inflation

Mar Bastero-Gil,<sup>1,\*</sup> Arjun Berera,<sup>2,†</sup> Ian G. Moss,<sup>3,‡</sup> and Rudnei O. Ramos<sup>4,§</sup>

<sup>1</sup>*Departamento de Física Teórica y del Cosmos, Universidad de Granada, Granada-18071, Spain*

<sup>2</sup>*SUPA, School of Physics and Astronomy, University of Edinburgh, Edinburgh, EH9 3JZ, United Kingdom*

<sup>3</sup>*School of Mathematics and Statistics, Newcastle University, NE1 7RU, United Kingdom*

<sup>4</sup>*Departamento de Física Teórica, Universidade do Estado do Rio de Janeiro, 20550-013 Rio de Janeiro, R.J, Brazil*

The theory and methodology is developed to compute the bispectrum in warm inflation, leading to results for the non-linearity parameter and the shape of the bispectrum. Particular attention is paid to the study of the bispectrum in the regime of weak dissipation and how stochastic fluctuations affect the bispectrum. It is shown that, in contrast to the strong dissipative regime, the amplitude of non-Gaussianity is strongly dependent on the parameters governing the microscopic physics in the intermediate and weak dissipation warm inflation regimes. The most important results concern the shape of the bispectrum, which has two different, but distinct, forms in the weak and strong dissipative regimes.

PACS numbers: 98.80.Cq

## I. INTRODUCTION

Inflation remains one of the most appealing solutions to the cosmological puzzles. Observations from the cosmic microwave background are consistent with density perturbations that are very close to Gaussian and scale invariant. Measurements on non-Gaussianity from the first year Planck data [1] show that they are severely constrained although there remains room that there could be a detectable signal.

There are two dynamical pictures of inflation that have been developed. In one the scalar inflaton field is pictured to be almost non-interacting with all other fields [2]. Thus, the Universe inflates in a vacuum state and the evolution of the scalar inflaton field is governed by zero temperature physics. This is the cold inflation picture. In the alternative picture, particle production occurs concurrent to inflationary expansion. The scalar inflaton field is governed by fluctuation-dissipation dynamics [3] that controls the seeds of density fluctuations. This is the warm inflation picture [4]. In this picture, for the simplest dynamics the seeds of density perturbation are thermal [3, 5, 6]. The interaction of the scalar field with other fields leads to particle production, which then leads to a dissipation and fluctuation term in the inflaton evolution equation [7, 8]. We should note that since its original proposal warm inflation has evolved quite considerably. Originally, dissipation was computed in the high temperature regime and it was soon realized that thermal corrections to the inflaton potential would spoil inflation [8, 9]. However, more recent model building realizations easily overcomes these early concerns about the implementation of the warm inflation idea (a detailed discussion of these issues and their solution is particularly discussed extensively, for example, in the review paper [10]). The basic idea is that dissipation is driven by the coupling of the inflaton to massive fields (with a mass larger than the temperature of the thermal bath), which in turn couple to light (relativistic) degrees of freedom. Therefore, in this regime thermal corrections to the effective potential are not an issue.

Recent findings reported by the BICEP2 collaboration [11] of a possible primordial tensor mode signal lead to a possible additional observable to help discriminate different inflation models as well as between these two paradigms of inflation. However, this alone may not be sufficient, since both paradigms have promising models for explaining a tensor mode at various energy scales. The most promising hope for discriminating between the two inflationary paradigms could come from measurement of non-Gaussianity. As the measurements of the cosmic microwave background (CMB) radiation becomes more and more precise, it is expected that not only will the magnitude for the non-Gaussianity be measured, but also be possible to determine its shape. In fact, more important than the magnitude of this effect would be the shape of the bispectrum. Large classes of inflation models can be described by different bispectrum shapes, as discussed in details in Ref. [12]. Among the various possibilities, warm inflation has its distinctive “warm” shape [13], which is very different from other more common shapes, like the equilateral, local, flat and others. In this paper we will develop the theory of non-Gaussianity in warm inflation building on the previous works starting with the first analysis of effects from the inflaton evolution equation [14], followed by an analysis of

\* mbg@ugr.es

† ab@ph.ed.ac.uk

‡ ian.moss@ncl.ac.uk

§ rudnei@uerj.br

the general relativity perturbation equations [13]. The latter paper in particular developed the theory for the regime where the dissipative coefficient is bigger than the Hubble scale, which has been referred to as strong dissipative warm inflation. In this paper we will develop the corresponding theory for when the dissipative coefficient is smaller than the Hubble scale, which is called weak dissipative warm inflation. Our work will also further develop the theory for the strong dissipative regime. In particular, a full analysis was recently done on all stochastic forces present during warm inflation and their effects on first-order cosmological perturbations [15]. In this paper we will look at all the second-order effects from all these sources of stochastic forces and, thus, their effect on non-Gaussianity in both the weak and strong warm inflation regimes.

Our results might be of importance in other contexts as well, such as non-Gaussianity in curvaton models and in those models where the curvature perturbations and the non-linearity is dependent on the details of the reheating dynamics. In addition any inflation scenarios involving particle production will in general have some form of backreaction dissipative effects, which necessarily will be accompanied also with fluctuation forces. All such scenarios basically follow the warm inflation picture. The details of these effects associated with the particle production can vary, but the general approach adopted in this paper would also apply to such circumstances.

This paper is organized as follows. In section II we review the fluctuations equations at first- and second-order for warm inflation. In section III we present the scheme developed to compute the bispectrum and the results for the non-linearity parameter. In section IV we study the shapes of the bispectrum for warm inflation. We present our conclusion in section V. Two appendices are included where we show some of the technical details.

## II. PERTURBATIONS: FIRST- AND SECOND-ORDER

Our aim is to analyse the non-Gaussianities generated by a mixture of a slow-rolling scalar field and a radiation fluid during warm inflation. We do this by constructing equations for a gauge invariant variable  $\Phi(k, t)$  and evaluating the second order contribution to the bispectrum,

$$B(k_1, k_2, k_3)\delta(\Sigma k) = \sum_{\text{cyc}} \langle \Phi_1(k_1, t_f)\Phi_1(k_2, t_f)\Phi_2(k_3, t_f) \rangle, \quad (2.1)$$

where ‘cyc’ denotes the set of cyclic permutations. The subscript in  $\Phi$  denotes first- and second-order perturbations, and the perturbations are evaluated at a final time  $t_f$  some e-folds after horizon crossing. We shall use the  $\zeta$ -variable [16], which can be defined in terms of the total density perturbation  $\delta\rho$  on surfaces of constant curvature by,

$$\Phi = \frac{\delta\rho}{3(p + \rho)}. \quad (2.2)$$

A large scale approximation, or the ‘delta N’ approach, can be used to show that this variable approaches a constant value on large scales [17, 18].

The second-order strategy follows previous work for bispectra in warm inflationary models [13, 19, 20], and focuses on contributions to the non-Gaussianity which are of order one in the slow-roll approximation. This makes it possible to discard many terms in the perturbation equations that are similar in size to the slow-roll parameters, in the way described below. We work in constant curvature gauge, dropping the metric perturbations. This is justified in the appendix A, where we show that the metric perturbations are of the same order as the slow-roll parameters.

In warm inflation, the inflaton field is coupled to radiation during inflation. We consider the situation where the radiation is close to thermal equilibrium, with temperature  $T$  and four-velocity  $u^\alpha$ . A covector  $n_\alpha$  is chosen orthogonal to the surfaces of constant time  $t$ , with spatial coordinates  $x^\alpha$  and spatial derivatives  $\partial_\alpha$ . The inflaton  $\phi$  satisfies a stochastic evolution equation with Gaussian noise term  $\xi$ ,

$$\ddot{\phi} + 3H\dot{\phi} + V_{,\phi}(\phi) + \Upsilon D\phi - \partial^2\phi = (2\Upsilon T)^{1/2}\xi, \quad (2.3)$$

where  $H = \dot{a}/a$  is the expansion rate and  $\partial^2 = a^{-2}\delta^{\alpha\beta}\partial_\alpha\partial_\beta$ . Dissipation effects are strongly influenced by the radiation, and they are evaluated in the rest frame of the fluid. The dissipation depends on a coefficient  $\Upsilon(\phi, T)$  and the derivative along the fluid four-vector  $D\phi = u^\alpha\nabla_\alpha\phi$  (in our notation latin indices mean space-time coordinates, while Greek ones refer to space components only).

Normal frame quantities will be used for the second-order theory. The ‘normal-frame’ approach used below closely follows ref. [21]. The fluid part of the stress-energy tensor is expressed in the form

$$T_{ab}^r = (p_r + \rho_r)n_a n_b + p_r g_{ab} + q_a n_b + q_b n_a + \Pi_{ab}, \quad (2.4)$$

where  $q_a$  and  $\Pi_{ab}$  are orthogonal to the normal direction. The scalar perturbations of the fluid in the normal frame are defined by the replacement

$$\rho_r \rightarrow \rho_r + \delta\rho^N, \quad (2.5)$$

$$p_r \rightarrow p_r + \delta p^N, \quad (2.6)$$

$$q_\alpha \rightarrow (1+w)\rho_r \delta v_\alpha^N, \quad \delta v_\alpha^N = \partial_\alpha \delta v^N. \quad (2.7)$$

These perturbations are expanded as a series, for example,

$$\delta\rho^N = \delta_1\rho^N + \delta_2\rho^N + \dots \quad (2.8)$$

The rest frame of the radiation fluid is called the energy frame, and the velocity perturbation in the energy frame is defined by

$$u_a = \gamma(n_a + \delta v_a^E), \quad (2.9)$$

where  $\gamma$  is the Lorentz factor. The density and pressure perturbations in the energy frame are  $\delta\rho^E$  and  $\delta p^E$ , and we take the standard relation for a radiation fluid:  $\delta p^E = \delta\rho^E/3$ . The first-order perturbations are the same in the energy or the normal frame, and  $\delta p^N = \delta\rho^N/3$ , but at second-order,

$$\delta_2\rho^N = \delta_2\rho^E + \frac{4}{3}\rho_r(\delta_1 v_\alpha^E)(\delta_1 v^{E\alpha}), \quad (2.10)$$

$$\delta_2 v_\alpha^N = \delta_2 v_\alpha^E + \frac{\delta_1 \rho^E}{\rho_r} \delta_1 v_\alpha^E, \quad (2.11)$$

$$\delta_2 \Pi_{\alpha\beta} = \frac{4}{3}\rho_r \left( \delta_1 v_\alpha^E \delta_1 v_\beta^E - \frac{1}{3} h_{\alpha\beta} \delta_1 v_\gamma^E \delta_1 v^{E\gamma} \right). \quad (2.12)$$

At the background level, the radiation fluid is sourced by the inflaton field  $\phi$  through a dissipation coefficient  $\Upsilon$ . In the slow-roll approximation ( $\dot{\phi}^2 \ll V(\phi)$ ,  $\ddot{\phi} \ll 3H\dot{\phi}$ ), we have:

$$\dot{\phi} \simeq \frac{-V_{,\phi}}{3H(1+Q)}, \quad (2.13)$$

$$\rho_r \simeq \frac{3}{4}Q\dot{\phi}^2, \quad (2.14)$$

where  $Q = \Upsilon/(3H)$  and again we have taken  $p_r = \rho_r/3$ .

To work with the fluctuations it is more convenient to use the following set of dimensionless quantities:

$$\zeta^\phi = H\delta\phi/\dot{\phi}, \quad (2.15)$$

$$\zeta^d = -\delta\dot{\phi}/\dot{\phi}, \quad (2.16)$$

$$\zeta^r = \delta\rho_r/4\rho_r, \quad (2.17)$$

$$\zeta^v = -H\delta v^r. \quad (2.18)$$

Note that  $\zeta^\phi$  and  $\zeta^v$  are, respectively, the field and radiation comoving curvature perturbation in the constant curvature gauge, while  $\zeta^r$  is the radiation curvature perturbation in the uniform density gauge.

The dissipation coefficient  $\Upsilon$  depends on the temperature and the scalar field [10, 22, 23]. But at leading order in the slow-roll approximation, only the temperature dependence  $\Upsilon \propto T^c$  is relevant:

$$\Upsilon^{-1}\delta_1\Upsilon = cT^{-1}\delta_1T = c\zeta_1^r, \quad (2.19)$$

where  $\zeta^r = \delta\rho^N/4\rho_r$ , and  $\rho_r \propto T^4$ . The second-order variation makes use of the relationship (2.10),

$$\Upsilon^{-1}\delta_2\Upsilon = c\zeta_2^r + c_2(\zeta_1^r)^2 - \frac{1}{3}cH^{-2}(\partial_\alpha\zeta_1^v)(\partial^\alpha\zeta_1^v), \quad (2.20)$$

where  $c_2 = c(c-4)/2$ . The frame transformations are also used for the second-order variation of  $D\phi = u^a\nabla_a\phi$ ,

$$\delta_2(D\phi) = \delta_2\dot{\phi} - H^{-1}(\partial^\alpha\zeta^v)(\partial_\alpha\delta_1\phi) + \frac{1}{2}H^{-2}(\partial_\alpha\zeta_1^v)(\partial^\alpha\zeta_1^v)\dot{\phi}. \quad (2.21)$$

The conserved total stress-energy tensor is given by that of the scalar field and the radiation fluid  $T_{ab} = T_{ab}^r + T_{ab}^{(\phi)}$ , and we can write

$$\nabla^a T_{ab}^r = J_b = -\nabla^a T_{ab}^{(\phi)}, \quad (2.22)$$

where  $J_a$  is interpreted as the flux of energy and momentum from the scalar to the fluid system [15]. After using eq. (2.3), we find

$$J_0 = \Upsilon D\phi\dot{\phi} - \sqrt{2\Upsilon T}\xi\dot{\phi}, \quad (2.23)$$

$$J_\alpha = \Upsilon\dot{\phi}\partial_\alpha\phi - \sqrt{2\Upsilon T}\xi\partial_\alpha\phi. \quad (2.24)$$

The noise terms in the energy-momentum flux vector were a new feature introduced in ref. [15]. We shall present results later for two cases, one with and one without the noise terms in the fluxes. This way we will be able to clearly see the effects that result from the noise term.

### A. First-order perturbations

If we drop the metric perturbations and the derivatives of the potential (see the appendix A), then the first-order inflaton equation in the normal frame (2.3) becomes

$$\delta_1\ddot{\phi} + 3H\delta_1\dot{\phi} + \delta_1(\tilde{\Upsilon}D\phi) - \partial^2\delta_1\phi = (2\tilde{\Upsilon}T)^{1/2}\xi, \quad (2.25)$$

where we have replaced  $\Upsilon$  by  $\tilde{\Upsilon} \equiv \tilde{\Upsilon}(\mathbf{k})$ , which includes the dependence of the dissipation coefficient on the momentum, as appropriate when treating perturbations instead of background quantities (see the appendix B for details). The radiation equation without the metric perturbations is

$$\delta_1\dot{\rho}^N + 4H\delta_1\rho^N + \frac{4}{3}\rho_r\partial^2\delta_1v^N = \delta_1J_0. \quad (2.26)$$

Similarly, the scalar velocity perturbation satisfies

$$\frac{4}{3}a^{-3}\{a^3\rho_r\delta_1v^N\}' + \frac{1}{3}\delta_1\rho^N = -\partial^{-2}\partial^\alpha\delta_1J_\alpha. \quad (2.27)$$

Using the dimensionless variables introduced in eqs. (2.15)-(2.18), the first-order fluctuation equations can be written in a compact form as:

$$L(a, H, \phi, \dots)\zeta^i = K^i\xi^i, \quad (2.28)$$

where  $L = H^{-1}\partial_t + \dots$ . The slow-roll approximation allows us to use the values of the fields at horizon crossing together with an expansion in slow-roll parameters  $\epsilon_X = d\ln X/Hdt$ . The leading-order slow-roll approximation is defined by setting  $\epsilon_X = 0$ , and then  $L$  depends only on the background values of the fields at horizon crossing and the value of  $k$ , in the combination  $z = k/(aH)$ . Furthermore, in constant curvature gauge, the metric fluctuations

are of order  $\epsilon_H$  times  $\zeta^i$  (at first and second perturbative order) and drop out of the equations for the fluctuations at leading-order in the slow-roll parameters (appendix A). Therefore, the dimensionless form of these equations at leading-order, in momentum space, are

$$H^{-1}\dot{\zeta}_1^\phi + \zeta_1^d = 0, \quad (2.29)$$

$$H^{-1}\dot{\zeta}_1^d + 3(1 + \bar{Q})\zeta_1^d - z^2\zeta_1^\phi - 3\bar{Q}c\zeta_1^r = -K^d\xi, \quad (2.30)$$

$$H^{-1}\dot{\zeta}_1^r - (c - 4)\zeta_1^r + 2\Gamma\zeta_1^d + \frac{1}{3}z^2\zeta_1^v = K^r\xi, \quad (2.31)$$

$$H^{-1}\dot{\zeta}_1^v + 3\zeta_1^v - \zeta_1^r - 3\Gamma\zeta_1^\phi = 0, \quad (2.32)$$

where:

$$\langle \xi(k, z)\xi(k', z') \rangle = H^{-2}a^{-3}(2\pi)^3\delta(k+k')\delta(t-t'). \quad (2.33)$$

As mentioned before, the dissipation coefficient carries a momentum dependence (appendix B),  $\bar{\Upsilon} \equiv \bar{\Upsilon}(\mathbf{k}) = \Gamma\Upsilon$ , where  $\Gamma \approx e^{-k/(2aT)}$ . This explicit momentum dependence is used in  $\bar{Q} = \Gamma Q$ . The dimensionless noise coefficients are

$$K^d = \frac{H\dot{\phi}}{\rho^{(\phi)} + p^{(\phi)}}(2\bar{\Upsilon}T)^{1/2}, \quad K^r = -\frac{H\dot{\phi}}{3(\rho_r + p_r)}(2\bar{\Upsilon}T)^{1/2}. \quad (2.34)$$

Note that the noise and damping terms become unimportant in the large-scale limit  $z = k/(aH) \rightarrow 0$ .

The gauge-invariant variable depends on the total density perturbation,

$$\delta_1\rho = \delta_1\rho^N + \dot{\phi}\delta_1\dot{\phi} + V_\phi\delta_1\phi, \quad (2.35)$$

to leading-order in the slow-roll parameters. The gauge-invariant variable can, therefore, be expressed in terms of the scalar and fluid variations, using  $p + \rho = (1 + Q)\phi^2$ ,

$$\Phi = \frac{Q}{1+Q}\zeta_1^r - \frac{1}{3}\frac{1}{1+Q}\zeta_1^d - \zeta_1^\phi. \quad (2.36)$$

At late times, when  $z \rightarrow 0$ , we have  $\zeta_1^B = -\zeta_1^\phi = -\zeta_1^v$ . However, the leading-order slow-roll approximation is valid for  $z^2 > \epsilon_H$ . The range of validity overlaps the large-scale regime ( $z < 1$ ), where the gauge invariant variables are constant. Therefore, we can solve the leading-order slow-roll equations and match the result on the large scale approximation in the range  $\epsilon_H^{1/2} < z < 1$ .

## B. Second-order perturbations

Similarly, if we drop the metric perturbations and the derivatives of the potential, then the second-order inflaton equation in the normal frame becomes

$$\delta_2\ddot{\phi} + 3H\delta_2\dot{\phi} + \delta_2(\Upsilon D\phi) - \partial^2\delta_2\phi = \delta_1K\xi^\phi. \quad (2.37)$$

The radiation equation is

$$\delta_2\dot{\rho}^N + 4H\delta_2\rho^N + \frac{4}{3}\rho_r\partial^2\delta_2v^N = \delta_2J_0. \quad (2.38)$$

Finally, the scalar velocity perturbation satisfies

$$\frac{4}{3}a^{-3}\{a^3\rho_r\delta_2v^N\} \cdot + \frac{1}{3}\delta_2\rho^N - \partial^{-2}\partial^\alpha\partial^\beta\delta_2\Pi_{\alpha\beta} = -\partial^{-2}\partial^\alpha\delta_2J_\alpha, \quad (2.39)$$

where  $\delta_2\Pi_{\alpha\beta}$  is given in eq. (2.12).

In the slow-roll approximation, the total second-order density perturbation is a combination of terms,

$$\delta_2\rho = \delta_2\rho^N + \dot{\phi}\delta_2\dot{\phi} + V_\phi\delta_2\phi + \frac{1}{2}(\delta_1\dot{\phi})^2 + (\partial_\alpha\delta_1\phi)(\partial^\alpha\delta_1\phi), \quad (2.40)$$

and the gauge invariant variable is given by

$$(1+Q)\Phi = Q\zeta_2^r - \frac{1}{3}\zeta_2^d - (1+Q)\zeta_2^\phi + \frac{1}{6}(\zeta_1^d)^2 + \frac{1}{3}H^{-2}(\partial_\alpha\zeta_1^\phi)(\partial^\alpha\zeta_1^\phi). \quad (2.41)$$

### III. BISPECTRUM: NUMERICAL SCHEME

Following the prescription for the first- and second-order perturbations discussed in the previous section, we find that the fluctuation equations can, therefore, be realized as a linear system of differential equations for a set of dimensionless fluctuating quantities  $\zeta^i$ . If we use  $\zeta_1^i$  for the first-order terms and  $\zeta_2^i$  for the second-order, then

$$L\zeta_1^i = K^i\xi^i, \quad (3.1)$$

$$L\zeta_2^i = j^i(k, \zeta_1, \xi), \quad (3.2)$$

where  $L = H^{-1}\partial_t + \dots$ . The source terms  $j^i$  can be read from the second-order equations given in the previous section. Sample source terms can be expressed in the simple forms,

$$c_1^i{}_{pq} \zeta_1^p \star \zeta_1^q, \quad (3.3)$$

$$c_2^i{}_{pq} k^{-2} (k^\alpha \zeta_1^p \star k_\alpha \zeta_1^q), \quad (3.4)$$

$$c_3^i{}_{pq} k^{-2} (\zeta_1^p \star k^2 \zeta_1^q), \quad (3.5)$$

$$c_4^i{}_{pq} K^i \zeta_1^p \star \xi^q, \quad (3.6)$$

$$c_5^i{}_{pq} k^{-2} k^\alpha (k_\alpha \zeta_1^p \star \xi^q), \quad (3.7)$$

where repeated  $p$  and  $q$  indices are summed. These coefficients are given explicitly in Table I.

$c_1^d{}_{dr} = -3cQ$	$c_1^d{}_{rr} = 3c_2Q$	$c_1^r{}_{dd} = 1$	$c_1^r{}_{dr} = -2c$	$c_1^r{}_{rr} = c_2$	
$c_2^d{}_{\phi v} = 3Q$	$c_2^d{}_{vv} = (c - 3/2)Q$	$c_2^r{}_{\phi v} = 1$	$c_2^r{}_{vv} = (c/3 - 1/2)$	$c_2^v{}_{\phi r} = 3c$	$c_2^v{}_{\phi d} = -3$
$c_3^v{}_{\phi r} = 3c$	$c_3^v{}_{\phi d} = -3$				
$c_4^d{}_{r\phi} = -c/2$	$c_4^r{}_{d\phi} = 1$				
$c_5^r{}_{r\phi} = -c/2$		$c_5^v{}_{\phi\phi} = -3$	$c_5^v{}_{rv} = -1/2$		

TABLE I. Coefficients of the quadratic terms in the second-order equations.  $c_2 = c(c-4)/2$ .

On large scales we use a gauge independent variable  $\Phi$ ,

$$\Phi_1 = c_i \zeta_1^i, \quad (3.8)$$

$$\Phi_2 = c_i \zeta_2^i + b_{ij} \zeta^i \star \zeta^j + e_{ij} k^{-2} (k^\alpha \zeta_1^i \star k_\alpha \zeta_1^j). \quad (3.9)$$

In the late time limit, it is always possible to choose  $c_i$  to be constant. For our particular choice of the gauge invariant variable, the coefficients  $c_i$ ,  $b_{ij}$ ,  $e_{ij}$  can be read from eqs. (2.36) and (2.41):

$$\begin{aligned}
c_r &= \frac{Q}{1+Q}, & c_d &= -\frac{1/3}{1+Q}, & c_\phi &= -1, \\
b_{dd} &= \frac{1/6}{1+Q}, \\
e_{\phi\phi} &= -\frac{z^2/3}{1+Q}.
\end{aligned} \tag{3.10}$$

A simple numerical scheme for calculating the bispectrum proceeds as follows. Choose a time  $t_f$  at which all the scales of interest have left the horizon. The bispectrum for the gauge invariant variables can be calculated from

$$B(k_1, k_2, k_3)\delta(\Sigma k) = \sum_{\text{cyc}} \langle \Phi_1(k_1, t_f)\Phi_1(k_2, t_f)\Phi_2(k_3, t_f) \rangle, \tag{3.11}$$

where ‘cyc’ denotes the set of cyclic permutations. We shall construct a differential equation for the bispectrum, which relates it to two-point correlation functions.

The first-order correlation of  $\Phi_1$  with  $\zeta_1^i$  is denoted by  $F^i$ ,

$$\langle \Phi_1(k_1, t_f)\zeta_1^j(k_2, t) \rangle = k_1^{-3}(2\pi)^3\delta(k_1 + k_2)F^j(k_1, t). \tag{3.12}$$

The power spectrum for  $\Phi$  is related to  $F^i$  by

$$P_\Phi(k) = k^{-3}c_i F^i(k, t_f). \tag{3.13}$$

Begin with the power spectrum calculation using eq. (3.1). By placing the system in a periodic box of length  $l$  it is possible to replace  $\delta(0)$  with  $l^3$ . Rescale the variables as follows,

$$\hat{\zeta}^i = (k/l)^{3/2}\zeta^i, \quad \hat{\xi}^i = (k/l)^{3/2}\xi, \tag{3.14}$$

then  $\hat{\xi}$  is a Gaussian random variable with

$$L\hat{\zeta}^i = K^i\hat{\xi}. \tag{3.15}$$

and from eq. (2.33),

$$\langle \hat{\xi}(k, t)\hat{\xi}(k, t') \rangle = k^3 a^{-3} H^{-2} \delta(t - t'). \tag{3.16}$$

The power spectrum is given by

$$P_\Phi(k) = k^{-3}c_i c_j \langle \hat{\zeta}^i(t_f)\hat{\zeta}^j(t_f) \rangle. \tag{3.17}$$

We also have correlation functions for  $\zeta^i$  and for the noise  $\xi^i$ ,

$$F^j(k, t) = c_i \langle \hat{\zeta}^i(k, t_f)\hat{\zeta}^j(k, t) \rangle, \tag{3.18}$$

$$F_\xi^j(k, t) = c_i K^j \langle \hat{\zeta}^i(k, t_f)\hat{\xi}^j(k, t) \rangle. \tag{3.19}$$

Note that all the dependence on the regularization scale  $l$  has dropped off from the equations.

The full bispectrum can be found by solving an ordinary differential equation. The first step is to split the gauge invariant perturbation into linear and quadratic parts,

$$\Phi_2 = \Phi_2^{(1)} + \Phi_2^{(2)}. \tag{3.20}$$

Define  $B^{(1)}(k_1, k_2, k_3, t)$  as follows,

$$B^{(1)}(k_1, k_2, k, t)\delta(\Sigma k) = \langle \Phi_1(k_1, t_f)\Phi_1(k_2, t_f)\Phi_2^{(1)}(k, t) \rangle. \quad (3.21)$$

From eq. (3.2), this satisfies

$$LB^{(1)}\delta(\Sigma k) = c_i \langle \Phi_1(k_1, t_f)\Phi_1(k_2, t_f)j^i(k, \zeta_1) \rangle. \quad (3.22)$$

The source terms are given by eqs. (3.3)-(3.7), and the expectation values decompose into products of correlation functions,

$$\begin{aligned} LB^{(1)} &= 2c_1c_2^i k_1^{-3}k_2^{-3}F^p(k_1, t)F^q(k_2, t) \\ &\quad + 2c_1c_2^i k_1^{-3}k_2^{-3}k^{-2}\mathbf{k}_1 \cdot \mathbf{k}_2 F^p(k_1, t)F^q(k_2, t) \\ &\quad + c_3c_3^i k_1^{-3}k_2^{-3}k^{-2} [k_2^2 F^p(k_1, t)F^q(k_2, t) + k_1^2 F^p(k_2, t)F^q(k_1, t)] \\ &\quad + c_4c_4^i k_1^{-3}k_2^{-3} [F^p(k_1, t)F_\xi^q(k_2, t) + F^p(k_2, t)F_\xi^q(k_1, t)] \\ &\quad + c_5c_5^i k_1^{-3}k_2^{-3}k^{-2}\mathbf{k}_3 \cdot [\mathbf{k}_1 F^p(k_1, t)F_\xi^q(k_2, t) + \mathbf{k}_2 F^p(k_2, t)F_\xi^q(k_1, t)]. \end{aligned} \quad (3.23)$$

The boundary conditions are  $B^{(1)} = 0$  at the initial time. The differential equation has to be solved for each set of momenta. Note that the equation for  $B^{(1)}$  has no stochastic source terms, and all the statistical averaging is already done when constructing  $F^p$ .

The remaining part of the bispectrum can be obtained directly,

$$B^{(2)}(k_1, k_2, k)\delta(\Sigma k) = b_{ij} \langle \Phi_1(k_1, t_f)\Phi_1(k_2, t_f)\zeta^i \star \zeta^j(k, t_f) \rangle + \dots \quad (3.24)$$

After decomposing the four-point function into correlators,

$$B^{(2)} = 2k_1^{-3}k_2^{-3} [b_{ij}F^i(k_1, t_f)F^j(k_2, t_f) + e_{ij}k^{-2}k_1 \cdot k_2 F^i(k_1, t_f)F^j(k_2, t_f)], \quad (3.25)$$

and the bispectrum is given by

$$B(k_1, k_2, k_3) = \sum_{\text{cyc}} [B^{(1)}(k_1, k_2, k_3, t_f) + B^{(2)}(k_1, k_2, k_3)]. \quad (3.26)$$

There is an important limitation of this result, which is caused by the use of the slow-roll approximation. We mentioned earlier that the fluctuations stabilize and the neglected slow-roll terms are small when  $\epsilon_H < z^2 < 1$ . This has to be true for all of the  $k$  values simultaneously, and so for example  $k_1 > k_2 \epsilon_H^{-1/2}$ . This cuts out the squeezed triangles with very small  $k_1$  (or  $k_2, k_3$ ). In the squeezed triangle limit, the argument of Maldacena [24] applies to warm inflation, and the bispectrum must be of the order of  $n_s - 1$ , where  $n_s$  is the spectral index. We will truncate the bispectrum for squeezed triangles.

The magnitude and shape of the bispectrum can be reduced to a non-linearity parameter  $f_{NL}$ , for which we take equilateral triangle shapes  $k_1 = k_2 = k_3$ , and a shape function  $B(k_1, k_2, k_3)$  that factors out from the equilateral triangle result [25]. In our variables,

$$f_{NL} = \frac{18}{5} \frac{B(k, k, k)}{P(k)^2}. \quad (3.27)$$

Different inflationary models predicts different shapes and magnitudes [12]. Observational constraints on  $f_{NL}$  depend on the shape template used. This is reflected in the latest Planck constraints on  $f_{NL}$  [1], for example

$$f_{NL}^{\text{local}} = 2.7 \pm 5.8, \quad f_{NL}^{\text{equi}} = -42 \pm 75, \quad f_{NL}^{\text{warm}} = 4 \pm 33. \quad (3.28)$$



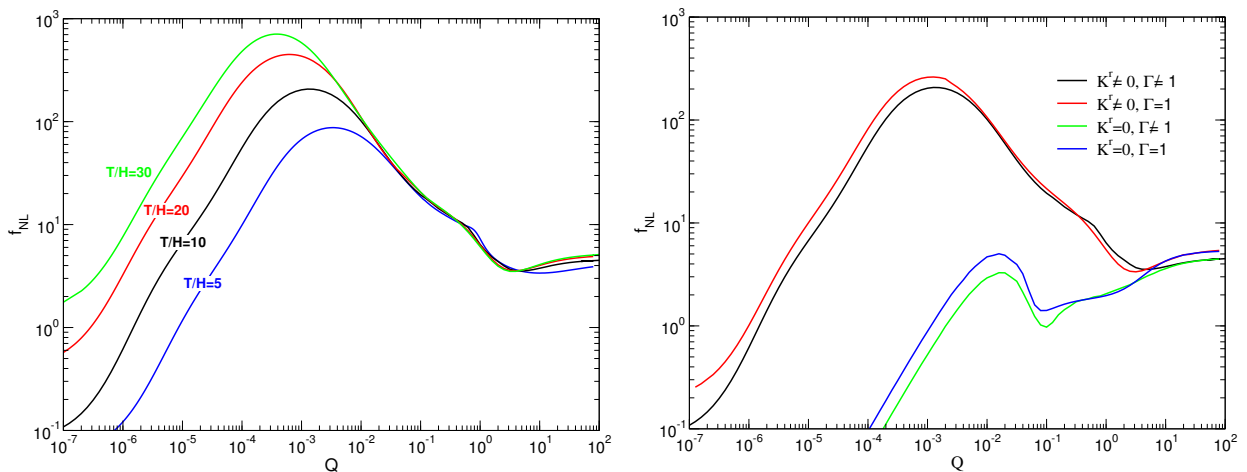


FIG. 1. LHS: Non-linearity parameter  $f_{NL}$  versus  $Q$  for different values of  $T/H$  as indicated in the plot. The dissipative coefficient includes a cut-off function when  $z \gg T$ , and the noise amplitude  $K^r$ . RHS: Comparison of  $f_{NL}$  when switching on/off the cut-off function  $\Gamma(z)$ , and the noise amplitude  $K^r$ , for  $T/H = 10$ .

These shapes are described in the next section.

In the case of warm inflation, using the slow-roll approximation, the theoretical prediction for the amplitude of the bispectrum depends only on the dissipative ratio  $Q = \Upsilon/(3H)$  and on the temperature of the thermal bath  $T/H$  at horizon crossing. In fig. 1 (LHS plot) we have plotted  $f_{NL}$  when varying  $Q$  for different values of  $T/H$ , and  $c = 3$ , i.e.,  $\Upsilon \propto T^3$ .

When  $Q \gtrsim 0.1$ , the level of non-Gaussianity is practically independent of  $T/H$ , and shows a very mild dependence on  $Q$  for  $Q > 1$ . Strong inflationary models, which are the ones with large  $Q$ , produce robust predictions for the non-Gaussianity, provided that  $c > 0$ . This behavior of  $f_{NL}$  is due to the presence of a “growing” mode in the spectrum for a  $T$ -dependent dissipative coefficient, which enhances the amplitude of the primordial spectrum by a factor  $Q^\alpha$ , [26, 27], and through the coupling of the radiation and field fluctuations enhances the bispectrum by a factor  $Q^{2\alpha}$  and, therefore, the effect partially cancels out in  $f_{NL}$ .

On the other hand, when  $Q$  is small there is a strong dependence on both  $Q$  and  $T/H$ . We have  $f_{NL} > 10$  for  $10^{-3} \lesssim Q \lesssim 10^{-1}$ , with the lower end for  $Q$  depending on  $T/H$ , and being, therefore, model dependent. Information on non-Gaussianity (combined with that of the primordial spectrum) can then be used in conjunction with model building to set constraints on the inflaton interactions.

The numerical result also shows that  $f_{NL}$  has a maximum at around  $Q \sim 10^{-3}$ , approximately at the value when dissipation starts dominating the primordial spectrum instead of the vacuum fluctuations [15]. For small values of  $Q \lesssim 0.1$ , we have for the amplitude of the primordial spectrum:

$$P_\zeta \simeq \left(\frac{H}{\dot{\phi}}\right)^2 \left(\frac{H}{2\pi}\right)^2 \left(80\pi\frac{T}{H}Q + 1\right), \quad (3.29)$$

and thermal fluctuations will start dominating at around  $Q \sim (H/T)/(80\pi)$ . Similarly, the bispectrum receives contributions from radiation fluctuations and inflaton vacuum fluctuations. The former goes as  $K^r \propto Q^{-1/2}$  (Eq. (2.34)) and thus grows towards small values of  $Q$ , giving a large contribution to the non-gaussianity. However this growth is reverted by the contribution from the vacuum fluctuations in the denominator of  $f_{NL}$ , giving rise to the peak observed in the plots.

On the RHS in fig. 1 we have compared different approximations for treating the radiation fluid perturbations, including or not both the momentum dependence function of the dissipation coefficient on the momentum,  $\Gamma(z)$ , and the noise term  $K^r$ . While at large  $Q$  the behavior of the fluctuations does not depend on these terms, it is relevant at low values of  $Q$ , the larger effect coming from the stochastic term in the radiation fluid  $K^r$ . This is useful to show the strong dependence of the non-Gaussianity on the microphysics of warm inflation in the intermediate and weak dissipation regime of warm inflation,  $Q \ll 1$ . We notice that when  $K^r = 0$ , the primordial spectrum for low  $Q$  is given by [15]:

$$P_\zeta \simeq \left(\frac{H}{\dot{\phi}}\right)^2 \left(\frac{H}{2\pi}\right)^2 \left(2\pi\frac{T}{H}Q + 1\right), \quad (3.30)$$

dissipation takes over vacuum fluctuations at slightly larger values of  $Q$ , and therefore the peak in  $f_{NL}$  is shifted towards the right (with a smaller value).

In fig. 2 we compare the value of  $|f_{NL}|$  for different values of  $c$  ( $\Upsilon \propto T^c$ ). The larger is  $c$ , the larger is the coupling between radiation and field fluctuations [26], which enhances the non-Gaussianity for  $Q \lesssim 1$ .

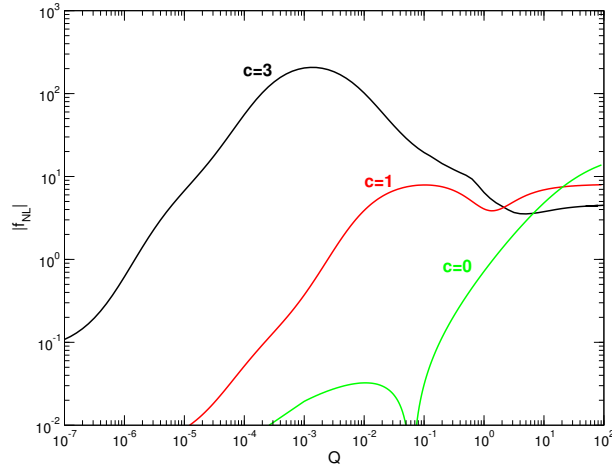


FIG. 2. Non-linearity parameter  $|f_{NL}|$  versus  $Q$  for different values of  $c$  ( $\Upsilon \propto T^c$ ) as indicated in the plot. The dissipative coefficient includes wavenumber dependent function  $\Gamma$  and the noise amplitude  $K^r$  (both explained in the text).

#### IV. FITTING BISPECTRAL SHAPES

The functional dependence of the bispectrum on the three momenta  $\mathbf{k}_1$ ,  $\mathbf{k}_2$  and  $\mathbf{k}_3$  is an important feature that can potentially distinguish different sources of non-Gaussianity and probe differences in inflationary models. Because of the condition  $\mathbf{k}_1 + \mathbf{k}_2 + \mathbf{k}_3 = 0$ , and the symmetry under permutations, the shape can be parameterized by parameters  $x_1 = k_1/k_3$  and  $x_2 = k_2/k_3$ , and  $k_3$  can be chosen to be the largest of the three wave-numbers. The triangle equality implies that  $x_1 + x_2 \geq 1$ . The plots in figure 3 show the numerical results of the dissipation coefficient  $Q$ .

Reconstruction of the bispectral shape from CMB observations is a difficult task and at present the best we might hope to do is compare different model bispectrum templates. We, therefore, require a template, or a set of templates, which are indicative of warm inflation models. Two such templates were identified in refs. [13, 19, 20] for the strong regime of warm inflation. One of these was the same local form [28] that is obtained from other inflationary models, such as curvaton models [29, 30],

$$B_L = \sum_{cyc} k_1^{-3} k_2^{-3}. \quad (4.1)$$

The other had the form

$$B_S = \sum_{cyc} k_1^{-3} k_2^{-3} (k_1^{-2} + k_2^{-2}) \mathbf{k}_1 \cdot \mathbf{k}_2, \quad (4.2)$$

which is specific to warm inflation. Note that the analytic treatment used in refs. [13, 19, 20] breaks down for squeezed triangles, and in practice we use a truncated form of  $B_S$  which is zero if any  $k_i < k_j \delta$ , with  $\delta \approx 0.1$  (of order of the slow-roll parameter).

Other bispectral shapes are suggested by the bispectrum equation (3.23). If  $F^p$  was constant, then the second source term would have the form

$$B_W = \sum_{cyc} k_1^{-3} k_2^{-3} k_3^{-2} \mathbf{k}_1 \cdot \mathbf{k}_2. \quad (4.3)$$

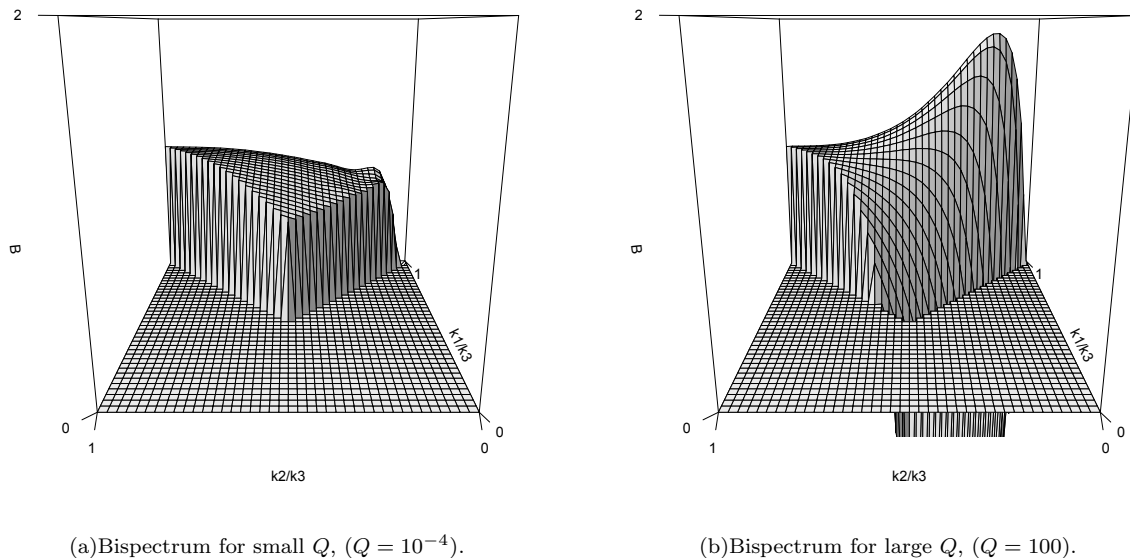


FIG. 3. The numerical spectrum plotted against  $x_1 = k_1/k_3$  and  $x_2 = k_2/k_3$ .

The first source term in eq. (3.23) has a local shape and the third term is a combination of the previous two when we use  $\mathbf{k}_1 + \mathbf{k}_2 + \mathbf{k}_3 = 0$ . These spectral shapes are plotted in figure 4. The fourth shape plotted in figure 4 is the equilateral template. This is similar to the warm inflation shape  $B_W$ , but an important difference is that the equilateral template vanishes when  $x_1 + x_2 = 0$ , unlike  $B_W$ .

For the weak regime of warm inflation ( $Q \ll 1$ ), we would like to find a simple representation of the numerical results obtained earlier, and find a template that is an optimal fit, in some sense, for different parameter ranges in  $Q$ , etc. Ideally, the comparison between different types of bispectral function should be done on a spherical projection using the angular components  $B_{l_1 l_2 l_3}$  (see, e.g., ref. [12]). This depends on the linear transfer function and is computationally expensive. A simpler approach is to use a momentum space comparison as, e.g., used in ref. [31]. Two spectral shapes with identical momentum dependence will give the same angular components, but the reverse is not necessarily true. The momentum space approach can be improved by modifications of the momentum space covariance function.

Matching the numerical bispectrum to a given template requires a distance function in bispectrum space, or equivalently, it requires an inner product or covariance function. This should respect the constraints and symmetries of the bispectrum. We start from an integral expression,

$$B_1 \cdot B_2 = \int d\mathbf{k}_1 d\mathbf{k}_2 d\mathbf{k}_3 \frac{B_1(k_1, k_2, k_3) B_2(k_1, k_2, k_3)}{P(k_1) P(k_2) P(k_3)} \delta(\mathbf{k}_1 + \mathbf{k}_2 + \mathbf{k}_3). \quad (4.4)$$

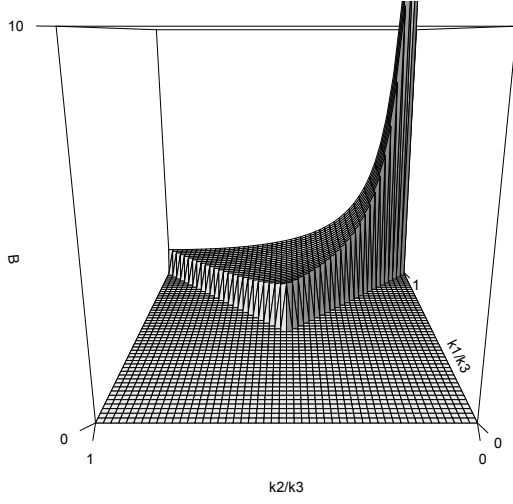
It is also possible to add any function  $\omega(k_1, k_2, k_3)$  that respects the symmetries of the integrand. The integral in eq. (4.4) then reduces to

$$B_1 \cdot B_2 = \frac{1}{8\pi^4} \int_{\Delta} dk_1 dk_2 dk_3 k_1 k_2 k_3 \frac{B_1(k_1, k_2, k_3) B_2(k_1, k_2, k_3)}{P(k_1) P(k_2) P(k_3)}, \quad (4.5)$$

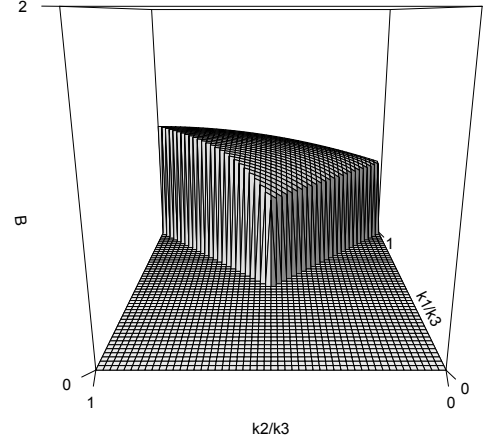
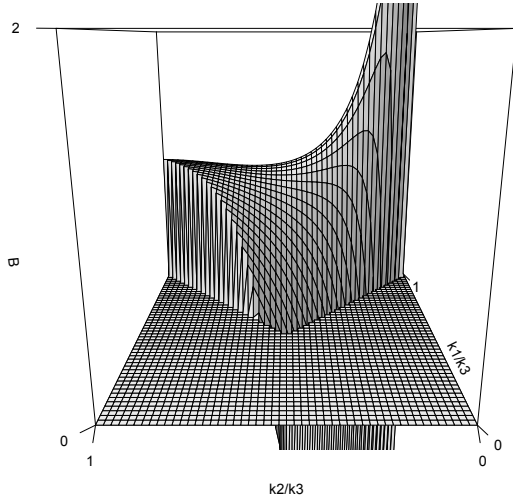
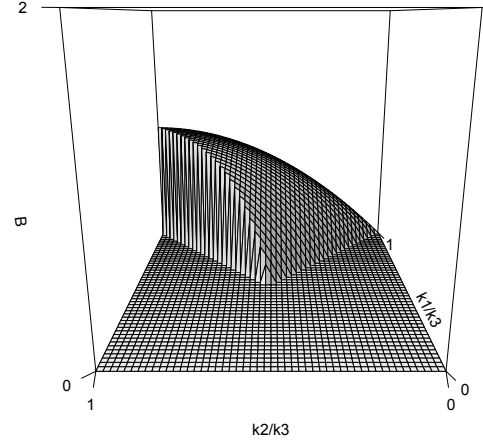
where  $\Delta$  is the range of the integral, restricted by the triangle inequality. At leading order in slow-roll, the spectra have approximate scaling symmetries of the form

$$B_1(k_1, k_2, k_3) = k_3^{-6} B(x_1, x_2, 1), \quad P(k) = k^{-3} P(1), \quad (4.6)$$

where  $x_1 = k_1/k_3$  and  $x_2 = k_2/k_3$ . In the new variables, after dropping an overall constant factor and re-instating the weight function, the integral becomes



(a)Local Bispectrum.

(b)Warm bispectrum type  $B_W$ .(c)Warm bispectrum type  $B_S$ .

(d)Equilateral bispectrum.

FIG. 4. Selected bispectral shapes plotted against  $x_1 = k_1/k_3$  and  $x_2 = k_2/k_3$ .

$$B_1 \cdot B_2 = \int_{1/2}^1 dx_1 \int_{1-x_2}^{x_2} dx_2 x_1^4 x_2^4 B_1(x_1, x_2, 1) B_2(x_1, x_2, 1) \omega(x_1, x_2). \quad (4.7)$$

The simplest choice  $\omega(x_1, x_2) = 1$  does not give convergence for some important bispectral shapes, and so we shall choose a simple truncation with cutoff  $\delta$ ,

$$\omega(x_1, x_2) = 0 \quad \text{for } x_1 < \delta \text{ or } x_2 < \delta, \quad (4.8)$$

$$\omega(x_1, x_2) = 1, \quad \text{otherwise.} \quad (4.9)$$

The suppression of the bispectrum for squeezed triangles is expected in models where the bispectrum is generated on sub-horizon scales [24]. The correlation function, or 'cosine', is defined as the normalized product,

$$\text{cor}(B_1, B_2) = \widehat{B}_1 \cdot \widehat{B}_2, \quad \widehat{B} = \frac{B}{\sqrt{B \cdot B}}. \quad (4.10)$$

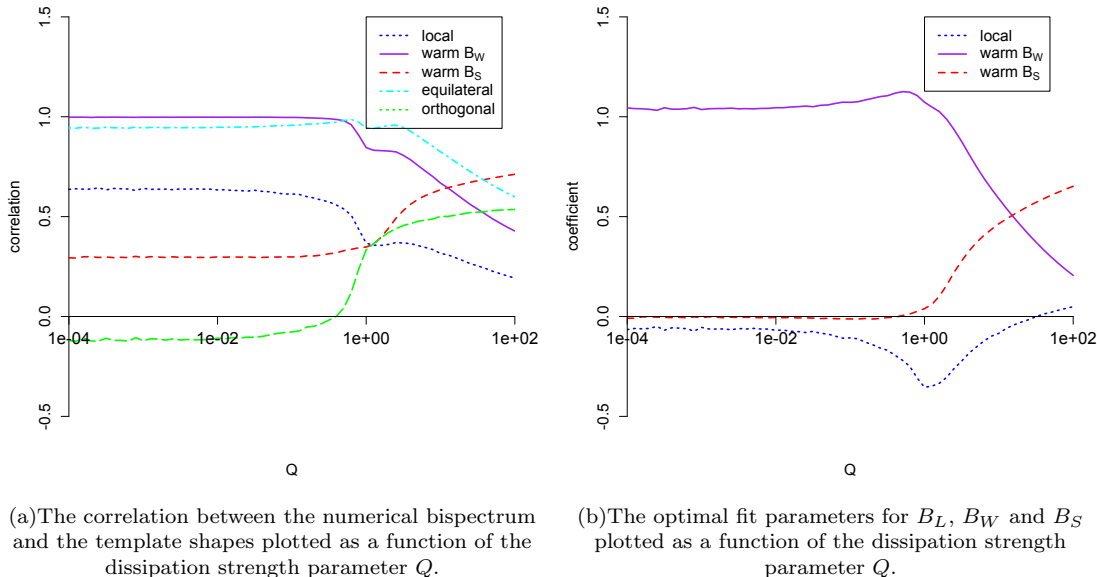


FIG. 5. Correlation between shapes as a function of the dissipation strength parameter  $Q$ .

The correlation function has been used in figure 5 (left-hand side panel) to compare the numerical bispectrum for the two warm templates  $B_S$  and  $B_W$  with those of the most common templates used in the literature, namely the local template  $B_L$ , the equilateral and the orthogonal shapes. There is a clear transition from the warm template  $B_W$  in the weak regime of warm inflation, where  $Q$  is small, to the warm template  $B_S$  in the strong regime of warm inflation, where  $Q$  is large. The correlation between the equilateral and  $B_W$  templates is quite large, approximately 0.94, and momentum space correlator cannot separate these two shapes efficiently.

The bispectrum can also be matched to a set of templates  $B_n$  with coefficients that minimize the residuals,

$$E(f_n) = \left( \widehat{B} - \sum_n f_n \widehat{B}_n \right)^2. \quad (4.11)$$

The square is taken using the inner product. The optimal fit has

$$f_n = \sum_m F_{nm}^{-1} \widehat{B}_m \cdot \widehat{B}, \quad (4.12)$$

where  $F_{nm}^{-1}$  is the inverse correlation matrix,  $F_{nm} = \widehat{B}_n \cdot \widehat{B}_m$ . A fit to the set  $B_L$ ,  $B_W$  and  $B_S$  is shown in figure 5 (right-hand side panel). The equilateral template has been left out because it has a large overlap with the  $B_W$  template. The numerical bispectrum is predominantly of the warm  $B_W$  form for small  $Q$  and of the  $B_S$  form for large  $Q$ .

## V. CONCLUSIONS

If primordial non-Gaussianity is observed, we will have a powerful new tool for distinguishing amongst the many different types of inflationary models. The warm inflationary models form a subclass of all inflationary models and can

produce a significant amount of non-Gaussianity in some parameter regimes. In the *strong* regime of warm inflation, the prediction for the non-linearity parameter is  $f_{NL} \approx 10$ , for models with a temperature dependent dissipation term. This is consistent, though slightly smaller, than the result predicted in ref. [19], which used crude analytic approximations.

In the *intermediate* regime of warm inflation, where  $Q \sim 1$ , the non-Gaussianity grows, but there is a proviso that the result depends on the effect of the stochastic dynamics on the heat flux. The  $f_{NL}$  parameter falls off for small values of the dissipation parameter  $Q$ , i.e., in the *weak* dissipation regime of warm inflation, and its amplitude also depends on the temperature of the thermal radiation bath. One should note that both the dissipation, temperature and the state for the inflaton fluctuations (thermal or quantum), strongly depend on the details of the interactions involved (see, e.g., refs. [32, 33]). Thus, the amplitude of non-Gaussianity for *weak* inflationary models is model dependent and is strongly dependent on the microscopic physics and dynamics.

The most important results we have found concern the shape of the bispectrum. The magnitude of the non-Gaussianity is an important observable, but the shape of the bispectrum has the potential of being even more relevant. The more common shapes, like the equilateral, local, flat, feature, etc., are useful to distinguish various different models of inflation. Nevertheless, many classes of inflation models can be described interchangeably by some of these shapes [1, 12]. Thus, even if one of these shapes turn out to be measured, there are still degeneracies among these inflation models that makes distinguishing models a difficult task. In this respect, warm inflation has specific shapes of its own, types  $B_W$  or  $B_S$  as we have shown.

The shape is different for the strong and weak regimes of warm inflation, but in both cases the shape is different from the shape of bispectrum obtained from any other inflationary model. The weak shape  $B_W$  is quite close to the equilateral shape, and so limits on  $f_{NL}$  for the equilateral shape are most likely relevant for this regime. The bispectral shape for the strong warm regime  $B_S$  agrees with previous analytic results, and this shape has a low correlation with other shapes. Our results show that there is a clear transition from the warm template  $B_W$ , which is the dominant shape in the weak regime of warm inflation ( $Q \lesssim 1$ ), to the warm template  $B_S$  in the strong regime of warm inflation ( $Q \gtrsim 1$ ). This is a novel result that has not been described in previous works.

There are some additional physical effects that can be included to refine the analysis. One of these is the possibility of viscosity (bulk and shear viscosities) in the radiation fluid (for studies of these effects in the perturbations at the first-order see, e.g., refs. [15, 27]). Viscosities would affect the amplitude of power spectrum, and could also have some effect on the bispectrum. Though fully including these effects in the second-order perturbation equations can be done along the lines of the study carried out in this work, it complicates considerably the analysis and we leave such study for a future work. Another important consideration is that the inflaton might be in a thermal state, adding an additional level of fluctuations beyond those induced from the thermal radiation. These fluctuations have been included in [15], for example. The inclusion of non-gaussianities arising from thermal field theory in such a situation is left for future work.

The results we have obtained in this paper may also be of relevance in contexts other than warm inflation. They can be of importance, for instance, in the studies of non-Gaussianities in curvaton type of models and where the curvature perturbations are generated during reheating after inflation [34, 35]. In these cases, both dissipation and stochastic noises in the radiation bath should be accounted for and they can be important in regards to the magnitude of  $f_{NL}$ . Recall, in particular, that from the results we have obtained here that radiation noise tends to enhance  $f_{NL}$ . This may potentially put additional pressure on curvaton type of models, which already tend to be in disagreement with the recent observational results [36].

## ACKNOWLEDGMENTS

M.B.G. is partially supported by “Junta de Andalucia” (FQM101). A.B. is partially supported by a UK Science and Technology Facilities Council Consolidated Grant. I.G.M. is partially supported by the UK Science and Technology Facilities Council Consolidated Grant ST/J000426/1. R.O.R. is partially supported by research grants from the brazilian agencies Conselho Nacional de Desenvolvimento Científico e Tecnológico (CNPq) and Fundação Carlos Chagas Filho de Amparo à Pesquisa do Estado do Rio de Janeiro (FAPERJ). We would like to thank the Higgs Center in Edinburgh (UK), and I.M. and M.B.G. the “Centro de Ciencias Benasque Pedro Pascual” (Spain), for its hospitality during the writing of this paper.

## Appendix A: Metric perturbations

The spacetime metric for a scalar-type of perturbation is given by

$$ds^2 = -(1 + 2\alpha)dt^2 - 2\beta_{,i}dt dx^i + a^2 (\delta_{ij}(1 + 2\varphi) + 2\gamma_{,ij}) dx^i dx^j. \quad (\text{A1})$$

The perturbed Einstein equations up to second-order can be found in the literature (see, e.g., refs. [21, 30, 37, 38]) and are given below. These imply that the first-order metric perturbations are first-order in the slow-roll parameter and the second-order metric perturbations are second-order in the slow-roll parameters. We shall give the results for  $\alpha$  as an example.

We make use of the shear  $\chi$  and perturbed expansion rate  $\kappa$ , define, respectively, by

$$\chi = a(\beta + a\dot{\gamma}), \quad (\text{A2})$$

$$\kappa = 3H\alpha - 3\dot{\varphi} - \partial^2\chi. \quad (\text{A3})$$

The first-order perturbations of the Einstein equations are then [39]

$$\partial^2\varphi_1 + H\kappa_1 = -4\pi G\delta_1\rho, \quad (\text{A4})$$

$$\kappa_1 + \partial^2\chi_1 = -12\pi G(\rho + p)\delta_1v, \quad (\text{A5})$$

$$\dot{\chi}_1 + H\chi_1 - \alpha_1 - \varphi_1 = 8\pi G\delta_1\Pi, \quad (\text{A6})$$

$$\dot{\kappa}_1 + 2H\kappa_1 + \partial^2\alpha_1 - 3(\rho + p)\alpha_1 = 4\pi G(\delta_1\rho + 3\delta_1p). \quad (\text{A7})$$

The density, pressure and shear perturbations are the sum of the fluid and scalar density and pressure perturbations. In constant curvature gauge,  $\varphi_1 = \varphi_2 = 0$ , these combine to give

$$\alpha_1 = \epsilon_H H\delta_1v, \quad (\text{A8})$$

$$\frac{\kappa_1}{3H} = \epsilon_H \frac{\delta_1\rho}{3(p + \rho)}, \quad (\text{A9})$$

$$\chi_1 = \partial^{-2}(3H\alpha_1 - \kappa_1), \quad (\text{A10})$$

where  $\epsilon_H = -\dot{H}/H^2 = 4\pi G(\rho + p)/H^2$ . Note that the right-hand sides of the first two equations above are the product of a slow-roll parameter with the Lukas and Curvature variables respectively. The corresponding metric perturbations are explicitly first-order in the slow-roll expansion. On large scales, for Fourier modes with  $k < aH$ , the shear contains a growing factor  $k^{-2}$  but remains first-order as a result of the Lukas and Curvature variables converging to the same constant value.

The second-order equations are much more complicated, and Noh and Hwang [21, 38] (in their ‘spatial  $C = 0$  gauge’ with  $\gamma = 0$  and  $\beta_{,\alpha} = \partial_\alpha\chi$ ) give an equation for  $\alpha_2$ , which is

$$\alpha_2 = \epsilon_H H\delta_2v + \frac{1}{3}H^{-1}(N_2 - N_0), \quad (\text{A11})$$

where

$$N_0 = -\frac{9}{2}H\alpha_1^2 + \alpha_1\partial^2\chi_1 + \frac{3}{2}H(\partial_\alpha\chi_1)(\partial^\alpha\chi_1), \quad (\text{A12})$$

and

$$N_2 = -\partial^{-2}\partial^\alpha(\alpha_1\partial_\alpha\kappa_1) - 3\epsilon_H\partial^{-2}\partial^\alpha(\alpha_1\partial_\alpha H\delta_1v) + \frac{3}{2}\partial^{-2}\partial^\alpha((\partial_\beta\alpha_1)(\partial_\alpha\partial^\beta\partial^{-2}(3H\alpha_1 - \kappa_1))) - \frac{1}{2}\partial^{-2}\partial^\alpha(\partial_\alpha\alpha_1(3H\alpha_1 - \kappa_1)). \quad (\text{A13})$$

It follows that  $\alpha_2$  is first-order in the slow-roll expansion, whilst  $N_2$  and  $N_0$  are second-order.

## Appendix B: Dissipation coefficient $\tilde{\Upsilon}$

The dissipation coefficient  $\tilde{\Upsilon}$  in warm inflation describes the way the inflaton transfers its energy to radiation degrees of freedom. Its explicit form depends on the details of the interactions involved. These include the direct coupling of the inflaton to other fields, but also of these with other degrees of freedom, which make the radiation bath. Details of successful interaction schemes were first reported in ref. [40] (for details of the quantum field theory derivation of these dissipation terms, see, e.g., refs. [10, 22, 23]). For example, for a typical coupling of the inflaton field  $\phi$  to other scalar fields  $\chi$  of the form  $g_\chi \phi \chi^2$ , we can define a nonlocal in both space and time dissipation term entering in the effective equation of motion for the inflaton as [41]

$$\tilde{\Upsilon}(\mathbf{k}, \omega) = \frac{g_\chi^2}{\omega n(\omega)} \int \frac{d^3 p}{(2\pi)^3} \int_{-\infty}^{\infty} \frac{d\omega'}{2\pi} n(\omega') n(\omega - \omega') \tilde{\rho}_\chi(\mathbf{p}, \omega') \tilde{\rho}_\chi(\mathbf{k} - \mathbf{p}, \omega - \omega'), \quad (\text{B1})$$

where  $n(\omega)$  is the Bose-Einstein distribution function and  $\tilde{\rho}_\chi(\mathbf{k}, \omega)$  is the spectral function for the  $\chi$  field,

$$\tilde{\rho}_\chi(\mathbf{k}, \omega) = \frac{4\omega_\chi(\mathbf{k})\Gamma_\chi(\mathbf{k}, \omega)}{[\omega^2 - \omega_\chi^2(\mathbf{k})]^2 + [2\omega_\chi(\mathbf{k})\Gamma_\chi(\mathbf{k}, \omega)]^2}, \quad (\text{B2})$$

where  $\omega_\chi(\mathbf{k})$  is the dispersion relation for the field  $\chi$  and  $\Gamma_\chi(\mathbf{k}, \omega)$  is its decay width. The explicit expression for  $\Gamma_\chi(\mathbf{k}, \omega)$  can be found, e.g., in ref. [22] for different couplings of  $\chi$  with (light) radiation fields.

The local approximation for the dissipation coefficient, as appropriate to describe the background evolution, is defined by taking the limit  $\omega \rightarrow 0$ ,  $\mathbf{k} \rightarrow 0$  in eq. (B1). In this local approximation,  $\tilde{\Upsilon}(\mathbf{k}, \omega) \rightarrow \tilde{\Upsilon}(0, 0) \equiv \Upsilon$ . The perturbation for the inflaton field, however, involves an explicit dependence on the (space) momentum. Thus, we cannot take the local limit in space,  $\mathbf{k} \rightarrow 0$ , in eq. (B1).

First-order perturbations are not so much sensitive to small scales (large wavenumbers), since it is mostly determined by those momentum modes corresponding to scales larger than the horizon ( $z \ll 1$ ). This justifies the use of a local approximation for the dissipation coefficient in previous works (e.g., in refs. [15, 26]). However, the (space) momentum dependence is particularly important in the evaluation of the non-Gaussianity, since it is most sensitive to the small scale physics (large momentum, or  $z \gtrsim 1$ ). Taking the time localization of the dissipation coefficient in eq. (B1), but keeping the space momentum contribution, the most important contribution when  $\mathbf{k} \neq 0$  comes from the decay width in eq. (B2). With the explicit expressions found, e.g., in refs. [22, 41], for light radiation fields coupled to the  $\chi$  field, we obtain that

$$\tilde{\Upsilon}(\mathbf{k}, \omega \rightarrow 0) \approx e^{-k/(2aT)} \Upsilon, \quad (\text{B3})$$

up to small (logarithmic) dependences on the coupling constant of the  $\chi$  field with the radiation fields. In Eq. (B3) we have used comoving momentum  $k \equiv |\mathbf{k}|$ . The above expression (B3) is the one we used in our calculations for the spectrum.

- 
- [1] P.A. R. Ade et al. [Planck Collab.], arXiv:1303.5084.
  - [2] A. H. Guth, Phys. Rev. **D23** (1981) 347; A. Albrecht, P. J. Steinhardt, Phys. Rev. Lett. **48** (1982) 1220; A. D. Linde, Phys. Lett. **B108** (1982) 389.
  - [3] A. Berera and L. -Z. Fang, Phys. Rev. Lett. **74** (1995) 1912.
  - [4] A. Berera, Phys. Rev. Lett. **75** (1995) 3218; Phys. Rev. **D55** (1997) 3346.
  - [5] I. G. Moss, Phys. Lett. B **154** (1985) 12.
  - [6] A. Berera, Nucl. Phys. B **585** (2000) 666.
  - [7] A. Berera, Phys. Rev. D **54** (1996) 2519.
  - [8] A. Berera, M. Gleiser and R. O. Ramos, Phys. Rev. D **58** (1998) 123508.
  - [9] J. Yokoyama and A. D. Linde, Phys. Rev. D **60** (1999) 083509 [hep-ph/9809409].
  - [10] A. Berera, I. G. Moss and R. O. Ramos, Rept. Prog. Phys. **72** (2009) 026901.
  - [11] P. A. R. Ade et al. [BICEP2 Collaboration], Phys. Rev. Lett. **112** (2014) 241101.
  - [12] J. R. Fergusson and E. P. S. Shellard, Phys. Rev. D **80** (2009) 043510; M. Liguori, E. Sefusatti, J. R. Fergusson and E. P. S. Shellard, Adv. Astron. **2010** (2010) 980523.
  - [13] I. G. Moss and C. Xiong, JCAP **0704** (2007) 007.



- [14] S. Gupta, A. Berera, A. F. Heavens and S. Matarrese, *Phys. Rev. D* **66** (2002) 043510; S. Gupta, *Phys. Rev. D* **73** (2006) 083514.
- [15] M. Bastero-Gil, A. Berera, I. G. Moss and R. O. Ramos, *JCAP* **1405** (2014) 004.
- [16] J. M. Bardeen, P. J. Steinhardt and M. S. Turner, *Phys. Rev. D* **28** (1983) 679.
- [17] D. Wands, K. A. Malik, D. H. Lyth and A. R. Liddle, *Phys. Rev. D* **62** (2000) 043527.
- [18] N. S. Sugiyama, E. Komatsu and T. Futamase, *Phys. Rev. D* **87** (2013) 023530.
- [19] I. G. Moss and T. Yeomans, *JCAP* **1108** (2011) 009.
- [20] I. G. Moss and C. Graham, *JCAP* **0711** (2007) 004.
- [21] H. Noh and J. -c. Hwang, *Phys. Rev. D* **69** (2004) 104011.
- [22] M. Bastero-Gil, A. Berera and R. O. Ramos, *JCAP* **1109** (2011) 033.
- [23] M. Bastero-Gil, A. Berera, R. O. Ramos and J. G. Rosa, *JCAP* **1301** (2013) 016.
- [24] J. M. Maldacena, *JHEP* **0305** (2003) 013.
- [25] E. Komatsu, D. N. Spergel and B. D. Wandelt, *Astrophys. J.* **634** (2005) 14.
- [26] C. Graham and I. G. Moss, *JCAP* **0907** (2009) 013.
- [27] M. Bastero-Gil, A. Berera and R. O. Ramos, *JCAP* **1107** (2011) 030.
- [28] D. S. Salopek and J. R. Bond, *Phys. Rev. D* **42** (1990) 3936.
- [29] D. H. Lyth and Y. Rodriguez, *Phys. Rev. Lett.* **95** (2005) 121302; D. H. Lyth and Y. Rodriguez, *Phys. Rev. D* **71** (2005) 123508.
- [30] N. Bartolo, S. Matarrese and A. Riotto, *JCAP* **0401** (2004) 003.
- [31] D. Babich, P. Creminelli and M. Zaldarriaga, *JCAP* **0408** (2004) 009.
- [32] R. O. Ramos and L. A. da Silva, *JCAP* **1303** (2013) 032.
- [33] S. Bartrum, M. Bastero-Gil, A. Berera, R. Cerezo, R. O. Ramos and J. G. Rosa, *Phys. Lett. B* **732** (2014) 116.
- [34] K. Ichikawa, T. Suyama, T. Takahashi and M. Yamaguchi, *Phys. Rev. D* **78** (2008) 063545.
- [35] G. Leung, E. R. M. Tarrant, C. T. Byrnes and E. J. Copeland, *JCAP* **1209** (2012) 008.
- [36] D. H. Lyth, arXiv:1403.7323 [hep-ph].
- [37] V. Acquaviva, N. Bartolo, S. Matarrese and A. Riotto, *Nucl. Phys. B* **667** (2003) 119.
- [38] J. -c. Hwang and H. Noh, *Phys. Rev. D* **76** (2007) 103527.
- [39] J. -c. Hwang and H. Noh, *Class. Quant. Grav.* **19** (2002) 527.
- [40] A. Berera and R. O. Ramos, *Phys. Rev. D* **63** (2001) 103509; *Phys. Lett. B* **567** (2003) 294.
- [41] A. Berera, I. G. Moss and R. O. Ramos, *Phys. Rev. D* **76** (2007) 083520.